

A new approach to formulation of complex fuel surrogates

Nawar Al-Esawi^{1,2*}, Mansour Al Qubeissi^{2,3}

¹*Faculty of Arts, Science and Technology, University of Northampton, Northampton, NN1 5PH, UK*

²*Institute for Future Transport and Cities, Coventry University, Coventry. CV1 5FB, UK*

³*Faculty of Engineering, Environment and Computing, Coventry University, Coventry, CV1 2JH, UK*

* Corresponding author: Nawar.Al-Esawi@northampton.ac.uk

1 Abstract

2 This paper presents a new approach to the formulation of fuel surrogates in application to gasoline,
3 diesel, and their biofuel blends (including blends of biodiesel/diesel and ethanol/gasoline). This new
4 approach, described as a 'Complex Fuel Surrogates Model (CFSM)', is based on a modified version of the
5 Multi-Dimensional Quasi-Discrete Model (MDQDM). The new approach is aimed to reduce the full
6 composition of fuel to a much smaller number of components based on their mass fractions to formulate
7 fuel surrogates. The formulated surrogates for gasoline and blended ethanol/gasoline fuels matched the
8 data of the full compositions of the same fuels for droplet lifetime, surface temperature, density, vapour
9 pressure, H/C ratio, molar weight and research octane number, using the CFSM. Also, the cetane number
10 and viscosity of diesel and biodiesel/diesel blends were mimicked by their suggested surrogates. The
11 results were verified, with up to 7.2% errors between the two sets of predicted droplet lifetimes:
12 surrogates and full compositions of fuels.

13 **Keywords:** Biodiesel; Combustion; Diesel; Ethanol; Fuel surrogates; Gasoline

14 1. Introduction

15 Commercial fuels are complex mixtures of many hydrocarbon components [1,2]. Due to the lack of
16 chemical data and the complexities of the combustion processes of these fuels (including heating,
17 evaporation and ignition), and the consequences of computationally-expensive models, surrogates (a
18 much smaller number of components) are introduced to match the physical and chemical behaviours of
19 the original fuel composition. A wide range of fuel surrogates have been formulated to emulate either
20 the physical or chemical behaviours of the full fuel compositions [3–12].

21 Due to the lack of chemical data and the limitations of the computational resources, in some studies (e.g.,
22 [13–16]), fuels were approximated with single components; e.g., diesel and gasoline fuels were

23 represented by n-dodecane and iso-octane, respectively. However, as the chemical mechanisms and the
24 computational efficiency became compatible for a wider range of components, researchers started to
25 approximate fuels by a reasonably higher number of components to mimic the desirable characteristics
26 of fuel.

27 Mati et al. [3] approximated diesel fuel by 5 components and the yielded kinetics of oxidation were in a
28 good agreement with those for diesel fuel. Sarathy et al. [5] suggested two surrogates for gasoline FACE
29 A (Fuel used in Advanced Combustion Engines, Type A) and FACE C. Surrogates of five and six
30 components were suggested for FACE A and FACE C gasoline fuels, respectively. A very good agreement
31 was obtained in [5] between the suggested surrogates and the real fuels for the predictions of their
32 ignition time delays, Research Octane Numbers (RONs), Motor Octane Numbers (MONs), Hydrogen to
33 Carbon ratios (H/C) and average Molar Weights (MWs) . The latter work was further advanced in [6] by
34 suggesting three different surrogates for gasoline FACE A and FACE C fuels, to match the physical and
35 chemical characteristics of these fuels. Good agreement was obtained between the actual fuel and one
36 of the suggested surrogates. For instance, the distillation curve was mimicked by a deviation of
37 approximately 5%. The auto-ignition of gasoline FACE F and its surrogates was investigated
38 experimentally in [11]. The suggested surrogate, which consists of 3 components, showed a good
39 agreement with the full composition of the same fuel.

40 In a recent study by Elwardany et al. [7], three surrogates consisting of 5, 6 and 7 components were
41 formulated to match the physical characteristics of the gasoline FACE A fuel. The five-component
42 surrogates showed an almost identical droplet surface temperature and lifetime compared to those
43 predicted for the full composition (19 components) of the gasoline FACE A fuel. Twenty diesel fuel
44 surrogates were suggested in [4] to match the thermophysical properties of diesel fuel. Five surrogates
45 were suggested in [8] for gasoline FACE I to match the heating and evaporation of the original fuel. Also,
46 the heating and evaporation of light naphtha and its suggested surrogates were examined in [9]. In the
47 latter study, the formulated surrogates matched the heating and evaporation characteristics of the full
48 compositions. In their recent study, Poulton et al. [17] formulated some surrogates to match the droplet
49 lifetime and surface temperature of kerosene fuel. Their suggested surrogates showed good agreement
50 with the experimental measurements.

51 There are two types of surrogates, namely, physical and chemical surrogates. Physical surrogates are
52 used to match the processes preceding the onset of combustion (droplet heating and evaporation);
53 while chemical surrogates are used to match the combustion characteristics of fuels [1]. To the best of
54 our knowledge, there has not been any study on formulating surrogates for bio-fossil fuel blends to
55 match both the physical and chemical characteristics of these fuels. In this study, we present a new
56 approach for the formulation of surrogates and examine them for heating and evaporation and some of
57 the main combustion characteristics. A modified version of the Multi-Dimensional Quasi-Discrete Model
58 (MDQDM) (the model was originally introduced in [18] and applied to gasoline, diesel and fuel blends
59 in [19,20]) is used to formulate the physical surrogates of gasoline FACE C, diesel, ethanol/gasoline
60 blends and biodiesel/diesel blends.

61 **2. The model**

62 In 2010, Sazhin [21] introduced a new approach for the simulation of bi-component fuel droplet heating
63 and evaporation, the so-called Discrete Multi-Component Model (DMCM). This model was based on an
64 analytical solution to the transient heat and mass transfer equations [22–24]. The main distinctive
65 feature of the DMCM was that it considered the impacts of species thermal conductivities and
66 diffusivities within the droplet to account for the temperature gradient and transient diffusion of species
67 and recirculation, using effective thermal conductivity and effective diffusivity models [25]. The
68 capability of the DMCM for predicting the droplet heating and evaporation was validated against
69 experimental data for multi-component fuel mixtures [26,27]. The DMCM approach was
70 computationally expensive when used for real applications (i.e., fuels containing 100s of components).
71 In response to this problem, the MDQDM was introduced in [18] to reduce the large number of
72 components with a much smaller number of representative components, the so-called Quasi-
73 Components (QCs). The number of atoms in these QCs is non-integer; hence the name.

74 The MDQDM uses the same analytical solutions as those used in DMCM for solving the heat and mass
75 transfer equations. The QCs are generated within each hydrocarbon and methyl-ester groups. These
76 components have non-integer carbon numbers (see [20,27] for more details). It is not possible to
77 formulate the physical surrogates of each fuel using these QCs, because they cannot be measured
78 experimentally for validation purposes and cannot be implemented into commercial CFD codes for the

79 prediction of combustion characteristics, due to the unavailability of their chemical mechanisms. In this
 80 paper, we propose a modified version of the MDQDM, described as a ‘Complex Fuel Surrogates Model’
 81 (CFSM), to generate actual components (with rounding half-up to the nearest integer carbon numbers)
 82 and formulate fuel surrogates. The carbon number of each Approximate Discrete Component (ADC)
 83 generated by the CFSM can be introduced as:

$$n_{im} = \left\lceil \frac{\sum_{am}^{bm} (n_{im} Y_{im})}{\sum_{am}^{bm} Y_{im}} \right\rceil \quad (1)$$

84 where m refers to the hydrocarbon group number in the fuel, n is the carbon number of the i^{th}
 85 component in group m , Y is the mass fraction of the i^{th} component in group m . In contrast to the original
 86 MDQDM (where the QC carbon number is a non-integer value, see Equation (6) in [18]), the nearest
 87 integer of the carbon number (ADC) is determined in Equation (1). Also, in contrast to the MDQDM, we
 88 use the mass fractions Y_{im} (instead of the molar fractions) to calculate the ADC group averaged carbon
 89 number n_{im} . These mass fractions are used to demonstrate the importance of heavy components on the
 90 expense of less important (lighter) ones for the prediction of droplet lifetime. For example, alkanes (the
 91 heaviest group) make up to 44.53% of diesel mass fractions (only 41.48% diesel molar fractions), which
 92 dominates the fuel composition on the expense of lighter components – such as naphthalenes with up
 93 to 7.46% mass fractions (9% molar fractions) and alkylbenzenes with up to 13.62% mass fractions
 94 (16.75 molar fractions).

95 The integer ADCs are generated within each group, where am and bm are the start and end counted
 96 components of the grouped species, respectively; and am for the second grouped components
 97 is bm_{old+1} . For example, a typical diesel fuel has 9 groups of hydrocarbons in which the group of alkanes
 98 contains 20 components. To reduce these 20 alkane components to 4 components, each 5 sequential
 99 components (sub-group) is grouped to form an ADC. The ADC carbon numbers of each sub-group of
 100 alkanes are determined as:

$$\left. \begin{aligned}
 n_{(1-5)m} &= \left[\frac{\sum_{i=5}^{i=1} (n_{im} Y_{im})}{\sum_{i=5}^{i=1} Y_{im}} \right] \\
 n_{(6-10)m} &= \left[\frac{\sum_{i=10}^{i=6} (n_{im} Y_{im})}{\sum_{i=10}^{i=6} Y_{im}} \right] \\
 n_{(11-15)m} &= \left[\frac{\sum_{i=15}^{i=11} (n_{im} Y_{im})}{\sum_{i=15}^{i=11} Y_{im}} \right] \\
 n_{(16-20)m} &= \left[\frac{\sum_{i=20}^{i=16} (n_{im} Y_{im})}{\sum_{i=20}^{i=16} Y_{im}} \right]
 \end{aligned} \right\} \quad (2)$$

101 Similarly, the ADC carbon numbers of the other groups are obtained.

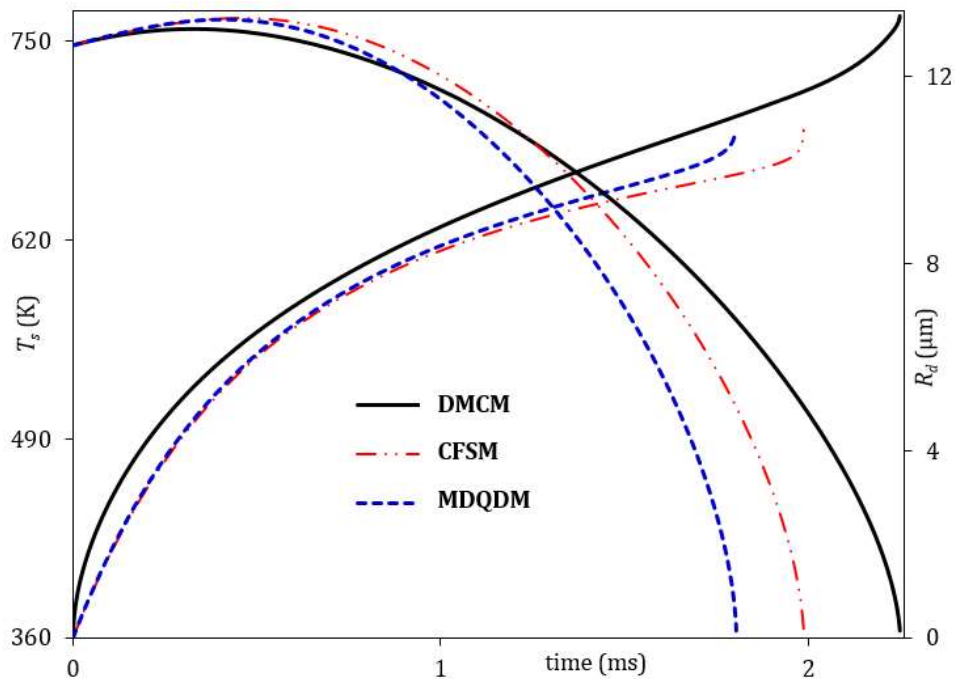
102 3. Diesel fuel surrogates

103 The diesel fuel surrogates were formulated using the CFSM, and their physical characteristics were
 104 compared with those predicted using MDQDM and DMCM. An example of the QCs generated using the
 105 MDQDM and the ADCs generated using the CFSM is presented in Table 1, where the 98 components of
 106 diesel fuel are replaced by 6 QCs and 6 ADCs.

107 Table 1. Quasi-Components (QCs) and Approximate Discrete Components (ADCs), representing the
 108 groups of species in diesel fuel.

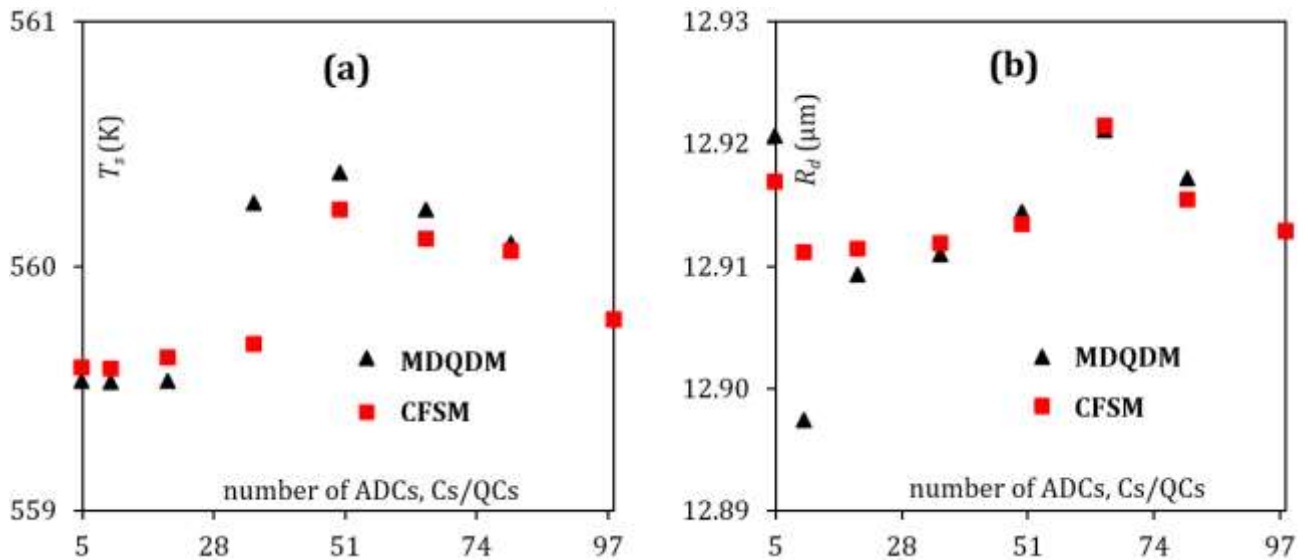
Group	Molar fractions (%)	QCs	Mass fractions (%)	ADCs
n-alkane	41.48	C _{14.763} H _{31.526}	44.53	C ₁₆ H ₃₄
cycloalkane	15.41	C _{15.364} H _{30.728}	17.05	C ₁₇ H ₃₄
bi-cycloalkane	7.89	C _{14.743} H _{27.486}	8.29	C ₁₆ H ₃₀
alkylbenzene	16.75	C _{11.726} H _{17.452}	13.62	C ₁₃ H ₂₀
tetraline	9.48	C _{13.832} H _{19.664}	9.05	C ₁₅ H ₂₂
naphthalene	8.99	C _{12.392} H _{12.784}	7.46	C ₁₃ H ₁₄

109
 110 Following [27], a diesel fuel droplet of initial radius $R_{do} = 12.66 \mu\text{m}$ and temperature $T_{do} = 360 \text{ K}$ was
 111 assumed to be moving at a constant velocity $U_d = 10 \text{ m} \cdot \text{s}^{-1}$ in still air. The ambient pressure and
 112 temperature were assumed equal to $p_g = 30 \text{ bar}$ and $T_g = 800 \text{ K}$, respectively. The evolutions of
 113 droplet radii predicted using the MDQDM and CFSM were compared to those of the full compositions of
 114 diesel fuel using the DMCM, as presented in Figure 1.



115
 116 Figure 1. Evolution of droplet surface temperatures and radii predicted for the full compositions of
 117 diesel fuel (98 components) using DMCM, 6 approximate discrete components (ADCs) using CFSM, and
 118 6 quasi-components (Qs) using MDQDM. The droplet velocity is $10 \text{ m} \cdot \text{s}^{-1}$ in still ambient air of
 119 pressure $p_g = 30 \text{ bar}$ and temperature $T_g = 800 \text{ K}$.

120 A detailed comparison between the MDQDM and CFSM was made at different time instants. The droplet
 121 radii and surface temperatures versus the numbers of Cs/QCs and ADCs were predicted using the
 122 MQDQM and CFSM at $t = 0.5 \text{ ms}$, $t = 1 \text{ ms}$, $t = 1.5 \text{ ms}$ and $t = 2 \text{ ms}$, as shown in Figures 2-5.



123
 124 Figure 2. The droplet surface temperatures (a) and radii (b) versus ADCs and Cs/QCs at time instant
 125 0.5 ms , using the same parameters as in Figure 1.

126
127

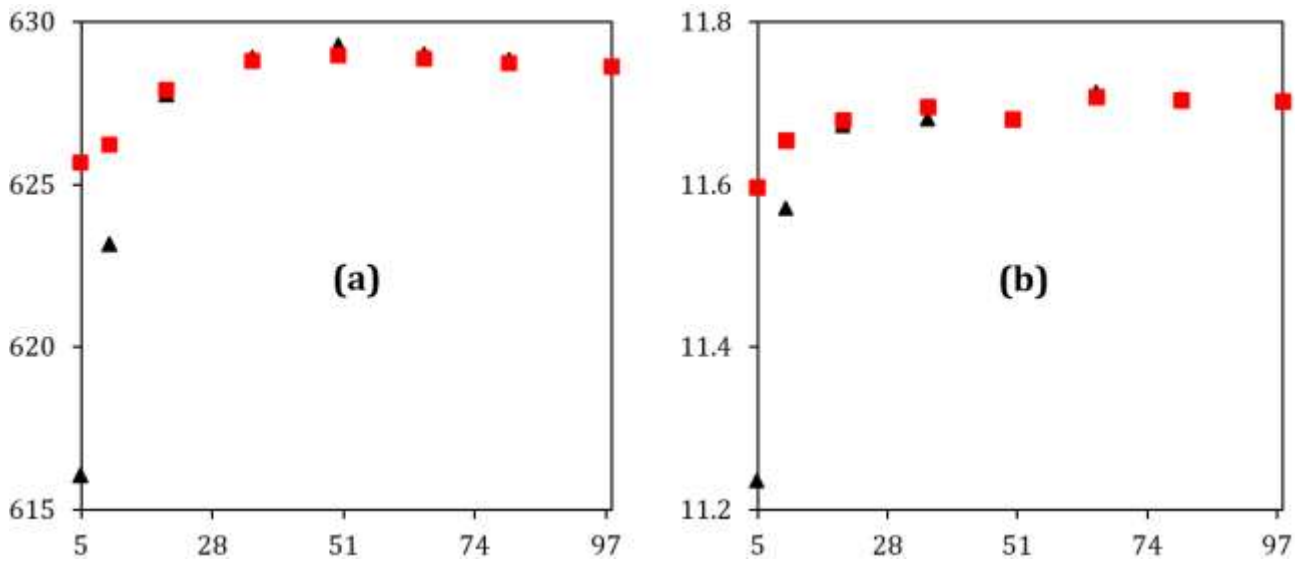


Figure 3. Same as Figure 2, but at time instant 1 ms.

128
129

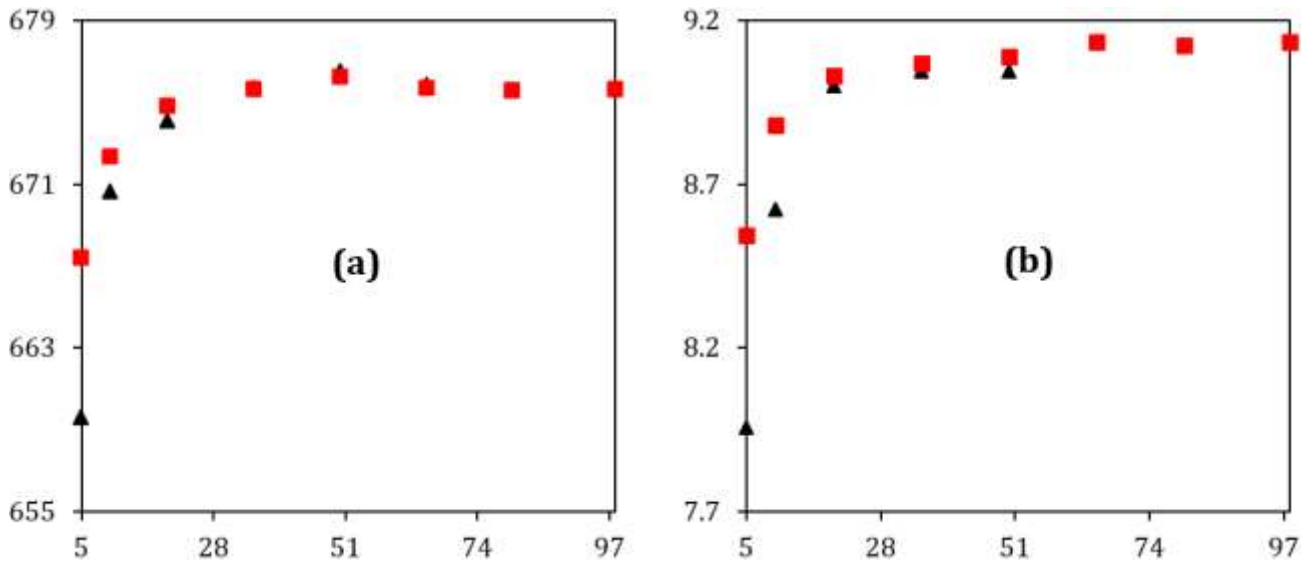


Figure 4. Same as Figures 2-3, but at time instant 1.5 ms.

130

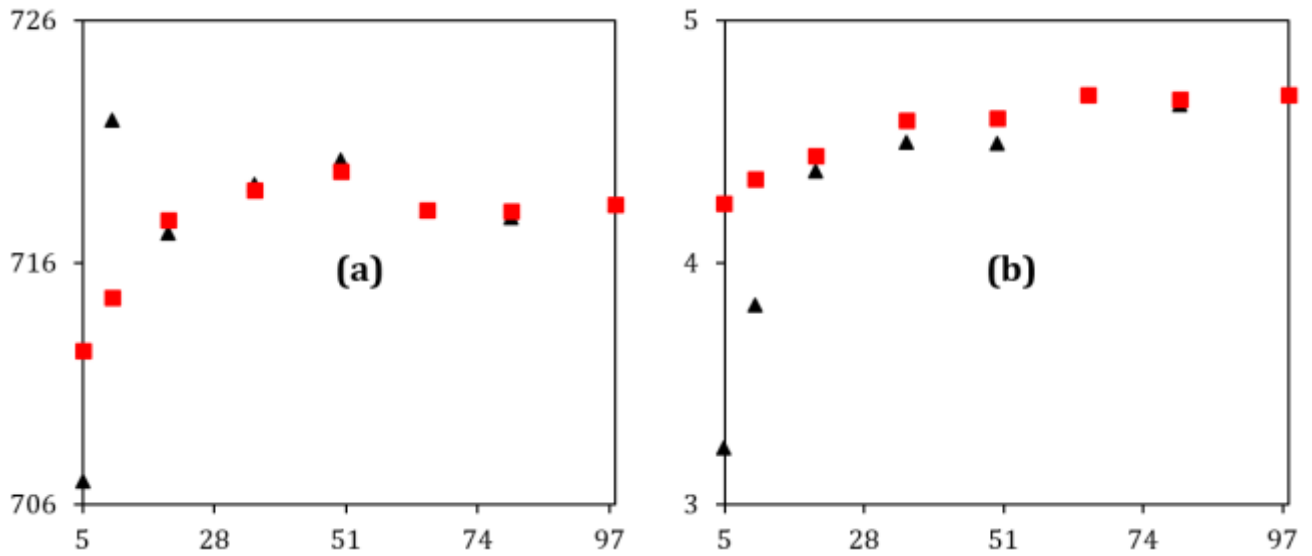


Figure 5. Same as Figures 2-4, but at time instant 2 ms.

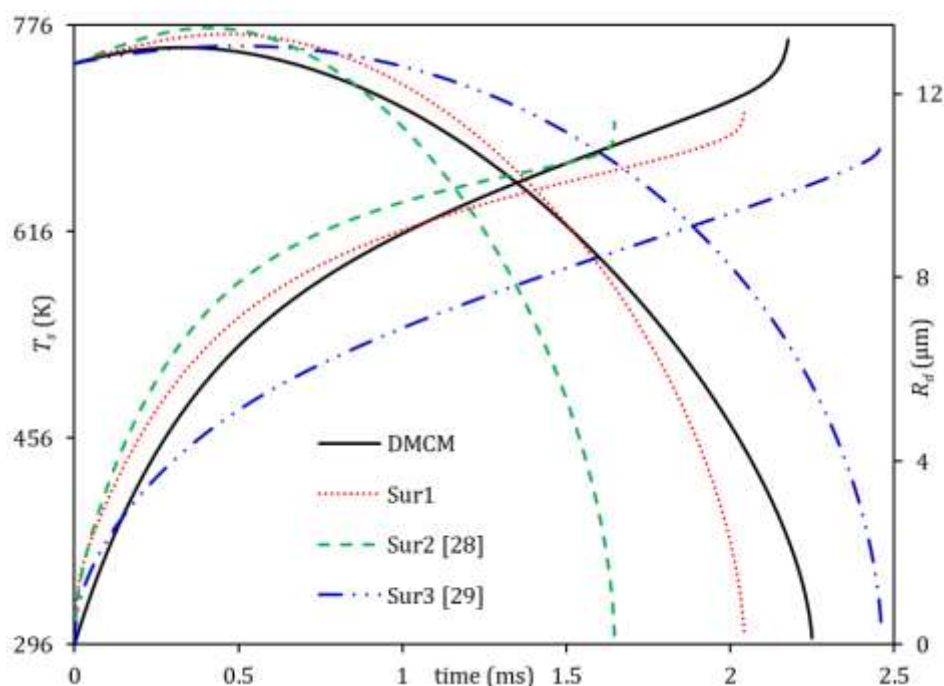
131
132

133 As can be seen from Figures 2-5, the predictions of CFSM are generally better than those obtained using
 134 the MDQDM especially with the small numbers (≤ 10) of ADCs and Cs/QCs. The predictions of the CFSM
 135 for droplet radii and surface temperatures when the full composition of diesel fuel (98 components) is
 136 approximated by 10 ADCs are reasonably close to those predicted using the DMCM with up to 4% errors.
 137 The results presented in Figures 2-5 confirm the previous trends inferred from Figure 1.
 138 Although the diesel droplet heating and evaporation using the CFSM are verified, the selection of ADCs
 139 in this model is still based on trial and error. Hence, this model still requires experienced end-users to
 140 run it. The impact of the trial and error on the predicted droplet surface temperatures and radii are
 141 noticeable in Figure 2 – where the new approximation of the full composition of diesel fuel with the
 142 range 50-75 ADCs overpredicts these results. Some fluctuations are observed in at different time
 143 instants (e.g., Figure 5) where those approximations can overpredict or underpredict the results of the
 144 98 components. A universal algorithm is undoubtedly needed for the selection of QCs or ADCs to
 145 minimise such uncertainty. In the current work, however, we aim to formulate fuel surrogates that
 146 match the real physical and chemical characteristics of their fuels. We have investigated the chemical
 147 and physical characteristics of our formulated diesel surrogates using the CFSM (Sur1) and two sets of
 148 surrogates from the literature (Sur2 [28] and Sur [29]), in comparison to those of the full composition
 149 of diesel fuel in [27]. Table 2 summarises the molar fractions of our formulated surrogates (Sur1) and
 150 the other two sets of surrogates (Sur2 and Sur3).

151 Table 2. The molar fractions of the three surrogates (Sur1, Sur2, and Sur3) of diesel fuel.

Component	Chemical formula	Molar fractions (%)		
		Sur1	Sur2 [28]	Sur3 [29]
n-hexadecane	C ₁₆ H ₃₄	42.89	41.3	0.88
iso-cetane	C ₁₆ H ₃₄	-	36.8	7.48
n-butylcyclohexane	C ₁₀ H ₂₀	-	-	29.66
n-pentylcyclododecane	C ₁₇ H ₃₄	16.43	-	-
bi-cyclohexane	C ₁₂ H ₂₄	-	-	25.26
bi-cyclooctane	C ₁₆ H ₃₀	7.89	-	-
toluene	C ₇ H ₈	-	-	10.94
heptylbenzene	C ₁₃ H ₂₀	13.12	-	-
decalin	C ₁₀ H ₁₈	-	-	25.78
1-dimethyl-4-iso-propyltetralin	C ₁₅ H ₂₂	8.72	-	-
naphthalene	C ₁₁ H ₁₀	-	21.9	-
1-methyl-2-ethyl-naphthalene	C ₁₃ H ₁₄	10.95	-	-

152 The diesel fuel droplet lifetimes were investigated for the full composition of fuel, using the DMCM and
153 the three surrogates (Sur1, Sur2 and Sur3) the evolutions of which are illustrated in Figure 6. The
154 droplet initial temperature was assumed equal to $T_{do} = 296$ K.



155 Figure 6. Evolutions of droplet surface temperatures and radii for the full compositions of diesel fuel
156 and its 3 surrogates (Sur1, Sur2 and Sur3), using the same parameters as in Figures 1-5 but for droplet
157 initial temperature equal to $T_{do} = 296$ K.
158

159 In Figure 6, the evolutions of droplet radii of Sur1 are of reasonably close with those predicted for the
160 full compositions of diesel, where it underpredicts the droplet's lifetime by only 7.2%. The predictions
161 of Sur2 (inferred from [28]) and Sur3 (inferred from [29]), however, can expose the predictions of
162 droplet lifetimes to errors up to 26.8% and 8.3%, respectively. Also, the droplet surface temperatures
163 are underpredicted by 7.3%, 8.4% and 9.9% using Sur1, Sur2 and Sur3 respectively. These errors are
164 estimated in comparison to the same values of the full composition of diesel fuel using the DMCM.

165 To further understand the suitability of the suggested surrogates to represent diesel fuel, the Cetane
166 Number (CN) was calculated for these surrogates. In the original composition of diesel fuel presented in
167 [18], n-alkanes and iso-alkanes were merged into one group due to their similar thermodynamic and
168 transport properties. For the calculation of CN, however, these two groups were treated individually in
169 our analysis, due to their different CN values with various component structures – normal (straight
170 chains) or isomers (branched chains) [30]. The viscosities of the two suggested surrogates were also
171 compared to the full compositions of diesel fuel. The viscosity is an important factor for the atomisation

172 and combustion processes [31,32]. It was predicted using the UNIFAC–VISCO method [33]. The
 173 predictions of the CNs and the viscosities of our formulated surrogates using the CFSM (Sur1) and the
 174 other two sets of surrogates (Sur2 and Sur3) were compared to those calculated for the full
 175 compositions of diesel fuel as shown in Table 3.

176 Table 3. The CNs and viscosities (in cP) of diesel fuel and its three surrogates (Sur1, Sur2 and Sur3).

Fuel	CN	Error (%)	Viscosity	Error (%)
diesel	54.5	-	4.516	-
Sur1	53.3	2.2	4.442	1.6
Sur2 [28]	39.8	27.0	4.483	0.8
Sur3 [29]	60.1	10.3	3.35	26.2

177

178 As can be seen from Table 3, Sur1 mimics the CN of diesel fuel with an error of less than 3%. Also, Sur1
 179 and Sur2 match the viscosity of the full composition of diesel fuel, but with errors of up to 1.6% and
 180 0.8%, respectively. As can be seen from these results (Figure 6 and Table 3), Sur2 model predictions are
 181 exposed to significant errors, beyond the acceptable limit. This is ascribed to the fact that Sur2
 182 (composed of 3 components) is dominated by alkanes (78.1%, as shown in Table 2), ignoring the fair
 183 contributions of other hydrocarbons. Considering the importance of physical and chemical features of
 184 fuel surrogates (droplet’s lifetime and temperature, CN and viscosity), Sur1 is relatively the best
 185 surrogate group to represent diesel fuel, compared with Sur 2 and Sur3 surrogates.

186 4. Gasoline fuel surrogates

187 The droplet surface temperature and lifetime for the full composition of gasoline FACE C were predicted
 188 in [19,26], assuming Raoult’s law was valid. In our previous study [34], the impact of activity coefficient
 189 on the vapour-liquid equilibrium for this fuel was accounted for. In this section, we present the
 190 comparison of the physical and chemical features of the full composition of fuel obtained from [19,26],
 191 our formulated surrogates using the CFSM (Sur4), and the two surrogates (Sur5 and Sur6) inferred from
 192 [5,6]. Table 4 illustrates the molar fraction of the three surrogates.

193 Table 4. The molar fractions of the three surrogates (Sur4, Sur5 and Sur6) of gasoline fuel.

Component	Molar fractions (%)		
	Sur4	Sur5 [5]	Sur6 [6]
n-butane	-	17.0	18.4

n-pentane	29.18	-	-
n-heptane	-	11.0	12.5
n-undecane	0.03	-	-
iso-pentane	10.74	8.0	5.0
iso-heptane	-	5.0	4.7
iso-octane	55.23	56.0	54.6
iso-decane	0.48	-	-
toluene	-	3.0	4.8
iso-propylbenzene	4.34	-	-

194

195

196

197

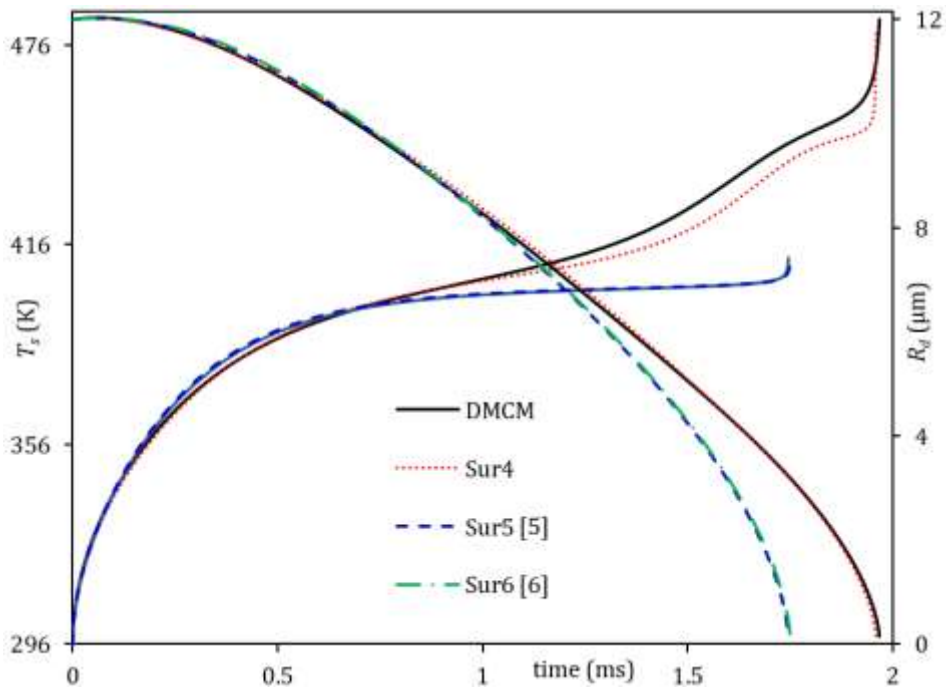
198

199

200

201

Initially, we predicted the droplet surface temperatures and lifetimes using DMCM. Following [26,34], the initial droplet radius was taken as equal to $R_{do} = 12 \mu\text{m}$, the droplet was at initial temperature $T_{do} = 296 \text{ K}$ and moving at a constant velocity $U_d = 24 \text{ m} \cdot \text{s}^{-1}$. The ambient gas (still air) pressure and temperature were assumed constant and equal to $p_g = 9 \text{ bar}$ and $T_g = 545 \text{ K}$, respectively. The predicted evolutions of droplet radii and surface temperatures for the full composition and the three surrogates are presented in Figure 7.



202

203

204

205

206

Figure 7. Evolutions of droplet radii and surface temperatures for the full compositions of gasoline and its 3 suggested surrogates: Sur4 (derived using the CFMS), Sur5 (inferred from [5]) and Sur6 (inferred from [6]). The droplet, with initial temperature $T_{do} = 296 \text{ K}$, was moving at $U_d = 24 \text{ m} \cdot \text{s}^{-1}$ in still ambient air of pressure $p_g = 9 \text{ bar}$ and temperature $T_g = 545 \text{ K}$.

207

208

209

As shown in Figure 7, the predictions of Sur4 droplet surface temperatures and radii, using the CFMS, are only 0.71% and 0.41%, respectively, less than those predicted for the full composition of the same fuel using the DMCM. At the same time, the use of the Sur5 and Sur6 surrogates underpredicts the

210 droplet lifetimes and surface temperatures by up to 15% and 11.3%, respectively. The densities and
 211 vapour pressures of the three fuel surrogates (Sur4, Sur5 and Sur6) and the full composition were
 212 calculated at the same input parameters and transient conditions of the droplet. The density of each
 213 component was predicted using the data inferred from [35]. The linear blending of volume fractions was
 214 used to make up the density of the mixture. The vapour pressure was calculated using the set of
 215 expressions provided in [33] for each component. The modified Raoult's law, using the UNIFAC model
 216 (see [34] for details), was used to determine the partial vapour pressure of each component. The
 217 predicted values of densities and vapour pressures for the full composition of fuel and the three fuel
 218 surrogates (Sur4, Sur5 and Sur6) are presented in Table 5.

219 Table 5. The calculated vapour pressures (in kPa) and densities (in $\text{kg} \cdot \text{m}^{-3}$) for gasoline fuel and its
 220 surrogates (Sur4, Sur5 and Sur6) at 296 K.

Fuel	Vapour pressure	Error (%)	Density	Error (%)
gasoline	34.25	-	682.3	-
Sur4	35.77	4.4	680.8	0.22
Sur5 [5]	54.49	59.1	680.3	0.29
Sur6 [6]	52.41	53.0	683.3	0.15

221
 222 As can be read from Table 5, the densities of all three surrogates are found to be in close agreement to
 223 that predicted for the full composition of gasoline fuel. However, the vapour pressures of the two
 224 surrogates, Sur5 and Sur6 (inferred from [5,6]), are found to be significantly different from those
 225 calculated for the full composition of gasoline fuel, showing errors of up to 59.1% and 53%, respectively.
 226 These large errors produced by Sur5 and Sur 6 surrogates were expected, because these surrogates
 227 were originally developed to match some ignition related factors (mainly, H/C, MW and RON) ignoring
 228 the physical processes (e.g., droplet lifetime and vapour pressure). We predicted these characteristics
 229 using Sur4, which provided only up to 4.4% errors, compared to the predictions of DCM.

230 The H/C ratio, MW and RON were compared to those of the full composition of gasoline FACE C.
 231 According to [36], the flame speed and the diffusivity of the real fuel can be matched using the suggested
 232 surrogates when the H/C ratio and the MWs are matched. Also, the ignition time delays of the fuel and
 233 its surrogates can be matched when their RONs are in good agreement [5]. The H/C ratios were
 234 predicted for the suggested surrogates using the following relationship [6]:

$$\frac{H}{C} = \frac{\sum_i^n X_i(N_{Hi})}{\sum_i^n X_i(N_{Ci})} \quad (3)$$

235 where X_i, N_{Ci}, H_{Ci} are the molar fraction, number of carbon atoms, and number of hydrogen atoms
 236 respectively, of their i^{th} component. The RON of Sur4 was predicted using the following relationship
 237 [37]:

$$RON = \frac{\sum_i v_i \beta_i ON_i}{\sum_i v_i \beta_i} \quad (4)$$

238 where v_i is the volume fraction of component i , β_i is a parameter value for each hydrocarbon group and
 239 ON_i is the octane number of component i . Equation 4 can be used for the predictions of RON and MON
 240 by using the appropriate β_i . The MW was calculated using the linear blending of the molar fractions.
 241 The values of RON, MW and the H/C ratio of the full composition fuel and the three surrogates are shown
 242 in Table 6. It should be emphasised that the RON, predicted in [5,6] for Sur5 and Sur6, were based on
 243 the linear molar blending rule and not on detailed hydrocarbon groups. As can be seen from this table,
 244 our suggested surrogates match the three aforesaid properties with negligible deviation compared to
 245 the full composition of FACE C gasoline fuel.

246 Table 6. The RONs, H/C ratios and MWs (in $\text{g} \cdot \text{mole}^{-1}$) of gasoline fuel and its surrogates.

Fuel	RON	H/C	MW
gasoline	84.7	2.27	97.2
Sur4	85.8	2.24	97.8
Sur5 [5]	85.3	2.25	98.4
Sur6 [6]	85.3	2.23	98.1

247

248 5. Blended ethanol-gasoline surrogates

249 The predictions of the droplet heating and evaporation of biodiesel, ethanol, ethanol/gasoline blends
 250 and biodiesel/diesel blends were investigated in [20,26,38–42]. Due to the interest in increasing the
 251 fraction of biofuels in the baseline fuel and to comply with some of the recent governmental regulations
 252 (for instance, the UK Department for Transport announced in April 2018 that the government was
 253 aiming to double the use of biofuel from its current 4.9% to 9.75% by 2020), the formulation of bio-
 254 fossil fuel blend surrogates is essential to study the feasibility of increasing the biofuel fractions. In a
 255 recent study, the isoamyl alcohol proved to be a suitable fuel to be blended with gasoline without any
 256 engine modifications [43]. Therefore, we have tried to formulate surrogates for ethanol/gasoline blends.

257 The ethanol/gasoline fuel surrogates were generated using the input parameters and ambient
 258 conditions described in section 4. The UNIFAC model was implemented for all functional groups in this
 259 section (without any approximation) due to the significant non-ideality of ethanol/gasoline blends. The
 260 impact of ethanol addition on droplet lifetime and surface temperature was presented in [26,34]. In this
 261 study, the impact of ethanol on the RON and the densities was investigated and compared to those of
 262 pure gasoline. In addition, the predictions of all the aforementioned characteristics were predicted by
 263 the suggested fuel surrogates and compared to the full composition of fuel. The RONs and the densities
 264 of different fractions of ethanol/gasoline blends are shown in Table 7 (EX is referred to X vol. % ethanol
 265 and (100-X) vol. % gasoline).

266 Table 7. The RONs and densities (in $\text{kg} \cdot \text{m}^{-3}$) of ethanol/gasoline fuel blends.

Fuel	RON	Density
gasoline	85.8	680.4
E5	87.7	685.7
E20	92.7	701.7
E50	100	773.8
E85	106	770.1
E100	108	787.2

267
 268 Results indicate that the addition of ethanol can be sacrificed in gasoline engines by up to 20% due to
 269 the minor deviations in RON and density (which were 8% and 3%, respectively) compared to pure
 270 gasoline. According to our findings in [34] and in the current work, ethanol can be blended with gasoline
 271 by up to 20% without any engine modifications. Based on these findings, the E20 was used for the
 272 surrogate formulation of the ethanol/gasoline blend. The molar fractions of our suggested surrogate,
 273 using the CFMS and the surrogates suggested in [44], are shown in Table 8.

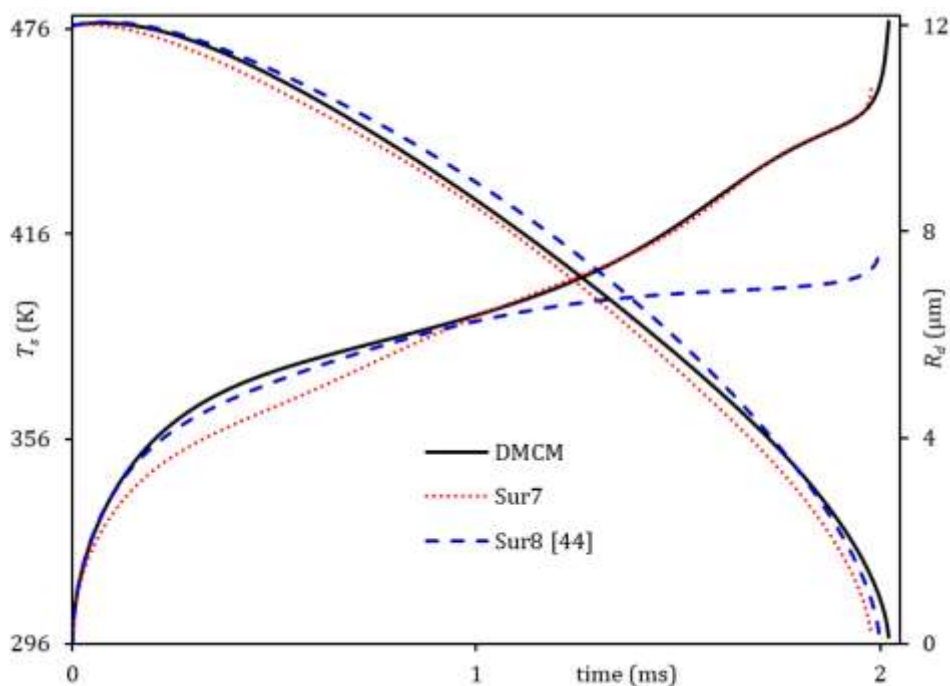
274 Table 8. The molar fractions of E20 surrogates (Sur7 and Sur8).

Component	Molar fractions (%)	
	Sur7	Sur8 [44]
n-hexane	18.13	-
n-heptane	-	11.82
iso-pentane	6.64	-
iso-octane	31.17	25.28
iso-decane	2.83	-

toluene	-	25.81
iso-propylbenzene	3.1	-
ethanol	38.13	37.08

275

276 The evolutions of the droplet radii and surface temperatures predicted by our formulated fuel
 277 surrogates (Sur7), the surrogates suggested in the literature (Sur8 [44]) and the full composition of the
 278 E20 blend, are shown in Figure 8.



279

280 Figure 8. Evolution of the droplet radii and surface temperatures for the full compositions of E20 and
 281 the two surrogates (Sur7 and Sur8).

282 The predictions reveal that our surrogates (Sur7) is in a good agreement with the full composition of
 283 E20. The predicted errors in droplet lifetime and surface temperature are up to 2.1% and 4%,
 284 respectively, compared to the same results predicted using the DMCM. Similarly, a negligible deviation
 285 in droplet lifetime, compared to the full composition of gasoline, is predicted for Sur8 (the surrogates
 286 inferred from [44]). However, using Sur8 shows a significant deviation in the droplet surface
 287 temperature with up to 14%. The RON, H/C and MW were studied to examine the ability of the two
 288 surrogates by means of fuel representation, as shown in Table 9. The RON, H/C and MW predicted by
 289 the two surrogates show a good agreement with those predicted by the full composition of gasoline fuel.

290

291

292 Table 9. The RONs, H/C ratios and MWs (in $\text{g} \cdot \text{mole}^{-1}$) of E20 fuel blends and its surrogates.

Fuel	RON	H/C	MW
E20	92.5	2.23	78.22
Sur7	95.3	2.24	79.54
Sur8 [44]	96.4	2.25	81.59

293

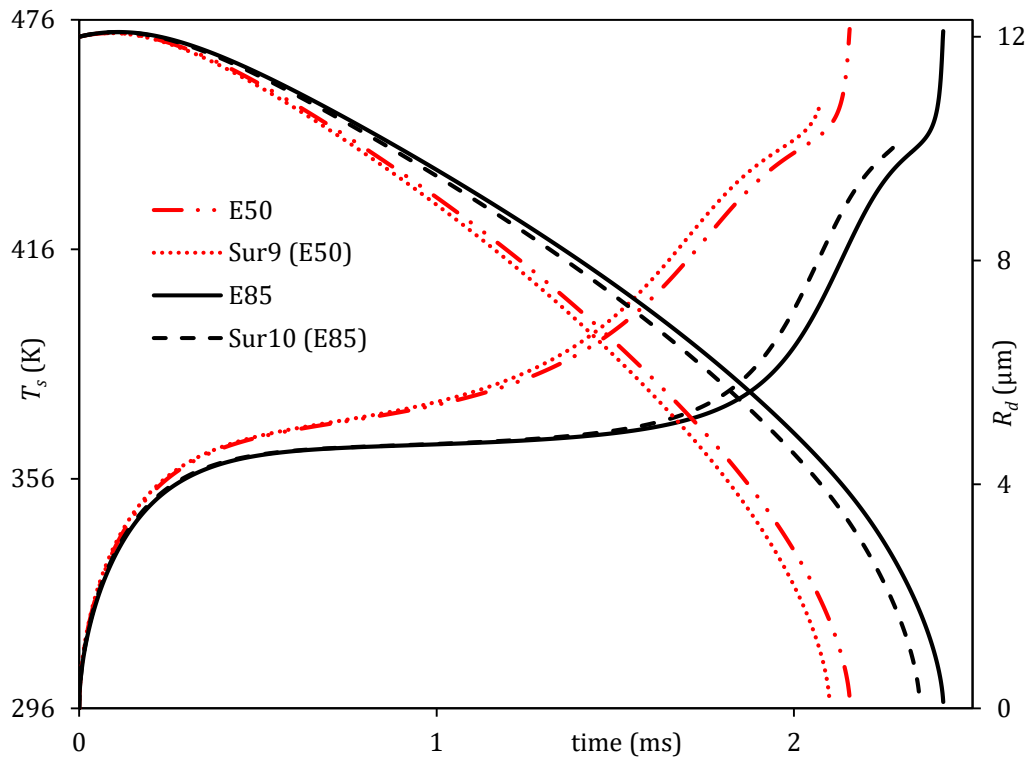
294 To further verify the CFSM ability to generate fuel surrogates, the E50 and E85 fuel blends of
295 ethanol/gasoline are examined. The molar fractions of the formulated surrogates of these two blends
296 (Sur9 for E50 and Sur10 for E85) are provided in Table 10.

297 Table 10. The molar fractions of Sur9 (surrogates of E50) and Sur10 (surrogates of E85).

Component	Molar fractions (%)	
	Sur9 (E50)	Sur10 (E85)
n-hexane	8.54	1.98
iso-pentane	3.09	0.72
iso-octane	14.54	3.37
iso-decane	1.32	0.31
iso-propylbenzene	1.45	0.33
Ethanol	71.15	93.29

298

299 The evolutions of droplet surface temperatures and lifetimes of the original composition of E50 and E85
300 fuel blends and their surrogates Sur9 and Sur10, respectively, are presented in Figure 9. Also, the RONs,
301 H/C ratios and MWs of these fuel blends and their surrogates (Sur9 and Sur10) are presented in Table
302 11. As evident from these figure and table, the formulated surrogates for both E50 and E85 blends
303 capture the original characteristics of the full compositions of both fuel blends.



304

305 Figure 9. Evolutions of the droplet radii and surface temperatures for the full compositions of E50 and
 306 E85 and their two surrogates (Sur9 and Sur10).

307 Table 11. The RONs, H/C ratios and MWs (in $\text{g} \cdot \text{mole}^{-1}$) of E50 and E85 fuel blends and their surrogates.

Fuel	RON	H/C	MW
E50	100.1	2.55	61.03
Sur9 (E50)	102.7	2.58	61.4
E85	106	2.85	49.55
Sur10 (E85)	107	2.85	49.61

308

309 6. Blended biodiesel-diesel surrogates

310 The feasibility of adding biodiesel fuel to diesel at different fractions has been highlighted in many
 311 studies (e.g., see [20]). Adding biodiesel to diesel can lead to a noticeable reduction in CO and smoke
 312 emissions [45,46]. According to the latest renewable fuel statistics report by the UK Department for
 313 Transport, 80% of the biodiesel produced in the UK was from used cooking oil, which accounts for
 314 around 115 million litres [47]. Therefore, biodiesel/diesel surrogates are commonly based on the blend
 315 of waste cooking oil biodiesel and diesel [48]. To the best of our knowledge, there is insufficient
 316 literature about the surrogates of Waste Cooking Oil (WCO) and its diesel blends. The impact of biodiesel
 317 addition on droplet lifetime and surface temperature was presented in [39]. In the current study, the
 318 impact of biodiesel on the CN was investigated and compared to that of pure diesel. The CN, predicted
 319 by different WCO biodiesel/diesel blends using the expression provided in our previous work [30]

320 which is based on the linear blending of volume fractions, is shown in Table 12. The original composition
 321 of WCO biodiesel fuel was inferred from [49].

322 Table 12. The CNs of biodiesel/diesel fuel blends.

Fuel	CN
diesel	54.5
B5	54.8
B10	55.1
B20	55.8
B50	57.7
B100	60.9

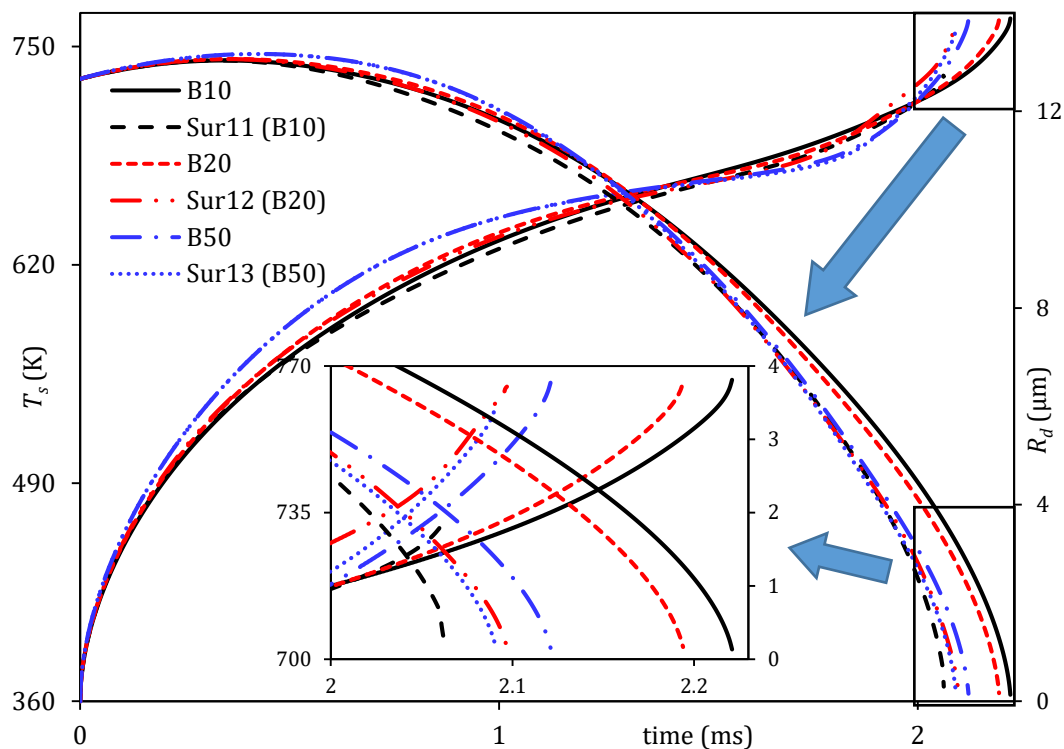
323 Following our recent finding in [39] and Table 12, biodiesel can be blended with diesel by up to 10%
 324 without a need for engine modification. In this section, we have used the same ambient conditions and
 325 input parameters as in Section 3 to generate surrogates of B10 (10% vol. biodiesel and 90% vol. diesel
 326 fuel blend), B20 and B50. We have examined the major physical and chemical fuel characteristics of the
 327 full compositions of B10, B20 and B50, compared with their formulated surrogates, Sur11, Sur12 and
 328 Sur13, respectively, using the CFSM. The molar fractions of these surrogates are presented in Table 13.

329 Table 13. The molar fractions of the B10, B20 and B50 surrogates (Sur11, Sur12 and Sur-13).

Component	Chemical formula	Molar fractions (%)		
		Sur11 (B10)	Sur12 (B20)	Sur13 (B50)
n-hexadecane	$C_{16}H_{34}$	38.60	34.31	21.44
n-pentylcyclododecane	$C_{17}H_{34}$	14.79	13.15	8.22
bi-cycloocatne	$C_{16}H_{30}$	7.09	6.30	3.94
heptylbenzene	$C_{13}H_{20}$	11.81	10.49	6.56
1-dimethyl-4-isopropyltetralin	$C_{15}H_{22}$	7.85	6.97	4.36
1-methyl-2-ethylnaphthalene	$C_{13}H_{14}$	9.86	8.78	5.48
1-methyl-oleate	$C_{19}H_{36}O_2$	5.85	11.71	29.25
1-methyl-linoleate	$C_{19}H_{34}O_2$	4.15	8.29	20.75

330
 331 The WCO fuel consists of 8 saturated components (making 24.1% of the fuel), 4 unsaturated components
 332 with one double bond (making 44.4% of the fuel) and 2 unsaturated components with two double bonds
 333 (making 31.5% of the fuel). Therefore, the dominant two groups are those with unsaturated methyl
 334 esters; hence the two dominant unsaturated components 1-methyl-oleate and 1-methyl-linoleate were
 335 chosen to represent WCO in B10, B20 and B50 fuel blend surrogates (Sur11, Sur12 and Sur13). The
 336 droplet radii and surface temperatures are predicted for Sur11, Sur12 and Sur13, using the CFSM, and
 337 compared with those of the full compositions of B10, B20 and B50 blends, using the DMCM, as shown in

338 Figure 10. As can be seen from this figure, the droplet lifetime and temperatures of the fuel surrogates
 339 are in good agreements with those predicted for the full compositions of their fuels. For instance, the
 340 surrogate droplet lifetimes and temperatures are underpredicted by up to 7.16% and 4.51%, compared
 341 with the full composition of B10. These underpredictions can be tolerated in some engineering
 342 applications.



343
 344 Figure 10. Evolutions of droplet radii and surface temperatures for the full compositions of B10, B20
 345 and B50 and their suggested surrogates.

346 The CN (predicted by the surrogate) is also compared to the full composition of B10. The CN of Sur11
 347 (53.9) shows a reasonable agreement with that of the full composition of B10 (55.1). Similarly, the CN
 348 predicted by the formulated surrogates of B20 (Sur-12) and B50 (Sur13) fuel blends show very good
 349 agreements with those predicted for the full compositions of the same fuel blends. We can conclude that
 350 the droplet lifetimes and surface temperatures and CN of our formulated surrogates (Sur11, Sur12 and
 351 Sur13) for the B10, B20 and B50 fuel blends match the full composition characteristics of these fuels.

352 7. Conclusion

353 The Multi-Dimensional Quasi-Discrete Model (MDQDM), based on the advanced Discrete Multi-
 354 Component Model (DMCM), was modified to formulate fuel surrogates using a new approach, described
 355 as a 'Complex Fuel Surrogates Model' (CFSM). The CFSM was verified against the DMCM, in application

356 to the full compositions of gasoline and diesel fuels and their ethanol/gasoline and biodiesel/diesel
357 blends. The main purpose of this work was to formulate accurate fuel surrogates and broaden the
358 usefulness of the model for future implementation into commercial CFD codes and experimental
359 validations. The physical and chemical properties of the formulated surrogates (Sur1 for diesel, Sur4 for
360 gasoline, Sur7 for E20, Sur9 for E50, Sur10 for E85, Sur11 for B10, Sur12 for B20, Sur13 for B50) were
361 compared to the full compositions of each fuel.

362 Our proposed surrogates were verified physically, in terms of their evolutions of droplet radii and
363 surface temperatures, and chemically, in terms of their chemical properties (e.g., H/C, research octane
364 numbers for gasoline and ethanol/gasoline fuels, and cetane numbers for diesel and biodiesel/diesel
365 fuels). The same physical and chemical verifications were applied to the fuel surrogates recommended
366 in literature (noting that the surrogates of biodiesel/diesel blend have not been presented anywhere in
367 literature to the best of our knowledge). The chemical and physical behaviours of our four surrogates
368 were in reasonably close agreements with those predicted for the full compositions of their fuels,
369 exceeding the relative predictions of these fuels provided by the surrogates suggested in literature. For
370 example, in the case of gasoline fuel the literature alternatives to Sur4 exposed the predicted droplet
371 lifetimes to errors of up to 26.8% and the predicted vapour pressure to errors of up to 59.1%. The
372 usefulness of the introduced CFM was verified for the formulation of surrogates in application to a
373 broad range of fuel compositions.

374 **Nomenclature**

375 **Abbreviations**

376	ADCs	approximate discrete components
377	B#	#% volume biodiesel/diesel fraction
378	CFD	computational fluid dynamics
379	CFM	complex fuel surrogate model
380	CN	cetane number
381	DMCM	discrete multi-component model
382	E#	#% volume ethanol/gasoline fraction
383	FACE	fuel used in advanced combustion engines
384	H/C	hydrogen/carbon
385	MDQDM	multi-dimensional quasi-discrete model
386	MON	motor octane number
387	MW	molar weight
388	ON	octane number
389	QCs	quasi-components
390	RON	research octane number

391	Sur#	surrogate number
392	UNIFAC	universal quasi-chemical functional-group activity coefficient
393	WCO	waste cooking oil
394	Symbols	
395	<i>m</i>	hydrocarbon group number
396	<i>n</i>	carbon number
397	<i>N</i>	number of atoms
398	<i>p</i>	pressure
399	<i>R</i>	radius
400	<i>t</i>	time
401	<i>T</i>	temperature
402	<i>U</i>	velocity
403	<i>v</i>	volume fraction
404	<i>x</i>	molar fraction
405	<i>y</i>	mass fraction
406	Greek symbol	
407	β	parameter value for octane number
408	Subscripts	
409	<i>C</i>	carbon
410	<i>d</i>	droplet
411	<i>g</i>	gas
412	<i>H</i>	hydrogen
413	<i>s</i>	droplet surface

Acknowledgment

The authors are grateful to the Institute for Future Transport and Cities, Coventry University (Project Ref. ECR019) for providing financial support for the work on this project.

References

- [1] Sarathy SM, Farooq A, Kalghatgi GT. Recent progress in gasoline surrogate fuels. *Progress in Energy and Combustion Science* 2018;65:67–108. <https://doi.org/10.1016/j.pecs.2017.09.004>.
- [2] Pitz WJ, Mueller ChJ. Recent progress in the development of diesel surrogate fuels. *Progress in Energy and Combustion Science* 2011;37:330–50. <https://doi.org/10.1016/j.pecs.2010.06.004>.
- [3] Mati K, Ristori A, Gail S, Pengloan G, Dagaut P. The oxidation of a diesel fuel at 1–10atm: Experimental study in a JSR and detailed chemical kinetic modeling. *Proceedings of the Combustion Institute* 2007;31:2939–46. <https://doi.org/10.1016/j.proci.2006.07.073>.
- [4] Lin R, Tavlarides LL. Thermophysical properties needed for the development of the supercritical diesel combustion technology: Evaluation of diesel fuel surrogate models. *The Journal of Supercritical Fluids* 2012;71:136–46. <https://doi.org/10.1016/j.supflu.2012.08.003>.
- [5] Sarathy SM, Kukkadapu G, Mehl M, Wang W, Javed T, Park S, et al. Ignition of alkane-rich FACE gasoline fuels and their surrogate mixtures. *Proceedings of the Combustion Institute* 2015;35:249–57. <https://doi.org/10.1016/j.proci.2014.05.122>.
- [6] Ahmed A, Goteng G, Shankar VSB, Al-Qurashi K, Roberts WL, Sarathy SM. A computational methodology for formulating gasoline surrogate fuels with accurate physical and chemical kinetic properties. *Fuel* 2015;143:290–300. <https://doi.org/10.1016/j.fuel.2014.11.022>.
- [7] Elwardany AE, Sazhin SS, Im HG. A new formulation of physical surrogates of FACE A gasoline fuel based on heating and evaporation characteristics. *Fuel* 2016;176:56–62. <https://doi.org/10.1016/j.fuel.2016.02.041>.
- [8] Elwardany A, Badra J, Sim J, Khurshid M, Sarathy M, Im H. Modeling of heating and evaporation of FACE I gasoline fuel and its surrogates, 2016, SAE 2016 World Congress and Exhibition. <https://doi.org/10.4271/2016-01-0878>.
- [9] Kabil I, Sim J, Badra JA, Eldrainy Y, Abdelghaffar W, Mubarak Ali MJ, et al. A surrogate fuel formulation to characterize heating and evaporation of light naphtha droplets. *Combustion Science and Technology* 2018;190:1218–31. <https://doi.org/10.1080/00102202.2018.1444037>.

- [10] Pati A, Gierth S, Haspel P, Hasse C, Munier J. Strategies to define surrogate fuels for the description of the multicomponent evaporation behavior of hydrocarbon fuels, 2018. <https://doi.org/10.4271/2018-01-1692>.
- [11] Kang D, Fridlyand A, Goldsborough SS, Wagon SW, Mehl M, Pitz WJ, et al. Auto-ignition study of FACE gasoline and its surrogates at advanced IC engine conditions. *Proceedings of the Combustion Institute* 2018. <https://doi.org/10.1016/j.proci.2018.08.053>.
- [12] Qian Y, Yu L, Li Z, Zhang Y, Xu L, Zhou Q, et al. A new methodology for diesel surrogate fuel formulation: Bridging fuel fundamental properties and real engine combustion characteristics. *Energy* 2018;148:424–47. <https://doi.org/10.1016/j.energy.2018.01.181>.
- [13] Sazhina EM, Sazhin SS, Heikal MR, Marooney CJ. The Shell autoignition model: applications to gasoline and diesel fuels. *Fuel* 1999;78:389–401. [https://doi.org/10.1016/S0016-2361\(98\)00167-7](https://doi.org/10.1016/S0016-2361(98)00167-7).
- [14] Sazhina EM, Sazhin SS, Heikal MR, Babushok VI, Johns RJR. A detailed modelling of the spray ignition process in diesel engines. *Combustion Science and Technology* 2000;160:317–44. <https://doi.org/10.1080/00102200008935806>.
- [15] Sileghem L, Alekseev VA, Vancoillie J, Van Geem KM, Nilsson EJK, Verhelst S, et al. Laminar burning velocity of gasoline and the gasoline surrogate components iso-octane, n-heptane and toluene. *Fuel* 2013;112:355–65. <https://doi.org/10.1016/j.fuel.2013.05.049>.
- [16] Davidson DF, Shao JK, Choudhary R, Mehl M, Obrecht N, Hanson RK. Ignition delay time measurements and modeling for gasoline at very high pressures. *Proceedings of the Combustion Institute* 2018. <https://doi.org/10.1016/j.proci.2018.08.032>.
- [17] Poulton L, Rybdylova O, Zubrilin IA, Matveev SG, Gurakov NI, Al Qubeissi M, et al. Modelling of multi-component kerosene and surrogate fuel droplet heating and evaporation characteristics: A comparative analysis. *Fuel* 2020;269:117115. <https://doi.org/10.1016/j.fuel.2020.117115>.
- [18] Sazhin SS, Al Qubeissi M, Nasiri R, Gun'ko VM, Elwardany AE, Lemoine F, et al. A multi-dimensional quasi-discrete model for the analysis of Diesel fuel droplet heating and evaporation. *Fuel* 2014;129:238–66. <https://doi.org/10.1016/j.fuel.2014.03.028>.
- [19] Al Qubeissi M, Sazhin SS, Turner J, Begg S, Crua C, Heikal MR. Modelling of gasoline fuel droplets heating and evaporation. *Fuel* 2015;159:373–84. <https://doi.org/10.1016/j.fuel.2015.06.028>.
- [20] Al Qubeissi M, Sazhin SS, Elwardany AE. Modelling of blended Diesel and biodiesel fuel droplet heating and evaporation. *Fuel* 2017;187:349–55. <https://doi.org/10.1016/j.fuel.2016.09.060>.
- [21] Sazhin SS, Elwardany A, Krutitskii PA, Castanet G, Lemoine F, Sazhina EM, et al. A simplified model for bi-component droplet heating and evaporation. *International Journal of Heat and Mass Transfer* 2010;53:4495–505. <https://doi.org/10.1016/j.ijheatmasstransfer.2010.06.044>.
- [22] Sazhin SS. Advanced models of fuel droplet heating and evaporation. *Progress in Energy and Combustion Science* 2006;32:162–214. <https://doi.org/10.1016/j.pecs.2005.11.001>.
- [23] Sazhin SS. *Droplets and Sprays*. London: Springer; 2014.
- [24] Sazhin SS. Modelling of fuel droplet heating and evaporation: Recent results and unsolved problems. *Fuel* 2017;196:69–101. <https://doi.org/10.1016/j.fuel.2017.01.048>.
- [25] Abramzon B, Sirignano WA. Droplet vaporization model for spray combustion calculations. *International Journal of Heat and Mass Transfer* 1989;32:1605–18. [https://doi.org/10.1016/0017-9310\(89\)90043-4](https://doi.org/10.1016/0017-9310(89)90043-4).
- [26] Al Qubeissi M, Al-Esawi N, Sazhin SS, Ghaleeh M. Ethanol/gasoline droplet heating and evaporation: Effects of fuel blends and ambient conditions. *Energy & Fuels* 2018;32:6498–506. <https://doi.org/10.1021/acs.energyfuels.8b00366>.
- [27] Al-Esawi N, Al Qubeissi M, Whitaker R, Sazhin SS. Blended E85–diesel fuel droplet heating and evaporation. *Energy & Fuels* 2019;33:2477–88. <https://doi.org/10.1021/acs.energyfuels.8b03014>.
- [28] Yu L, Mao Y, Li A, Wang S, Qiu Y, Qian Y, et al. Experimental and modeling validation of a large diesel surrogate: Autoignition in heated rapid compression machine and oxidation in flow reactor. *Combustion and Flame* 2019;202:195–207. <https://doi.org/10.1016/j.combustflame.2019.01.012>.
- [29] Huang Z, Xia J, Ju D, Lu X, Han D, Qiao X, et al. A six-component surrogate of diesel from direct coal liquefaction for spray analysis. *Fuel* 2018;234:1259–68. <https://doi.org/10.1016/j.fuel.2018.07.138>.
- [30] Al-Esawi N, Al Qubeissi M, Kolodnytska R. The Impact of biodiesel fuel on ethanol/diesel blends. *Energies* 2019;12:1804. <https://doi.org/10.3390/en12091804>.
- [31] Tse H, Leung CW, Cheung CS. Investigation on the combustion characteristics and particulate emissions from a diesel engine fueled with diesel-biodiesel-ethanol blends. *Energy* 2015;83:343–50. <https://doi.org/10.1016/j.energy.2015.02.030>.
- [32] Labeckas G, Slavinskas S, Mažeika M. The effect of ethanol–diesel–biodiesel blends on combustion, performance and emissions of a direct injection diesel engine. *Energy Conversion and Management* 2014;79:698–720. <https://doi.org/10.1016/j.enconman.2013.12.064>.
- [33] Poling BE, Prausnitz JM, O'Connell JP. *The Properties of Gases and Liquids*. New York: McGraw-Hill; 2001.

- [34] Al-Esawi N, Al Qubeissi M, Sazhin SS, Whitaker R. The impacts of the activity coefficient on heating and evaporation of ethanol/gasoline fuel blends. *International Communications in Heat and Mass Transfer* 2018;98:177–82. <https://doi.org/10.1016/j.icheatmasstransfer.2018.08.018>.
- [35] Yaws CL. *Transport Properties of Chemicals and Hydrocarbons: Viscosity, Thermal Conductivity, and Diffusivity of C1 to C100 Organics and Ac to Zr Inorganics*. Norwich, NY: William Andrew; 2009.
- [36] Mannaa O, Mansour MS, Roberts WL, Chung SH. Laminar burning velocities at elevated pressures for gasoline and gasoline surrogates associated with RON. *Combustion and Flame* 2015;162:2311–21. <https://doi.org/10.1016/j.combustflame.2015.01.004>.
- [37] Ghosh P, Hickey KJ, Jaffe SB. Development of a detailed gasoline composition-based octane model. *Industrial & Engineering Chemistry Research* 2006;45:337–45. <https://doi.org/10.1021/ie050811h>.
- [38] Al Qubeissi M. Predictions of droplet heating and evaporation: An application to biodiesel, diesel, gasoline and blended fuels. *Applied Thermal Engineering* 2018;136:260–7. <https://doi.org/10.1016/j.applthermaleng.2018.03.010>.
- [39] Al-Esawi N, Al Qubeissi M, Sazhin SS. The impact of fuel blends and ambient conditions on the heating and evaporation of diesel and biodiesel fuel droplets. 16th International Heat Transfer Conference, Beijing, China: Begellhouse; 2018, p. 6641–8. <https://doi.org/10.1615/IHTC16.mpf.020772>.
- [40] Bader A, Keller P, Hasse C. The influence of non-ideal vapor–liquid equilibrium on the evaporation of ethanol/iso-octane droplets. *International Journal of Heat and Mass Transfer* 2013;64:547–58. <https://doi.org/10.1016/j.ijheatmasstransfer.2013.04.056>.
- [41] Járvas G, Kontos J, Hancsók J, Dallos A. Modeling ethanol–blended gasoline droplet evaporation using COSMO-RS theory and computation fluid dynamics. *International Journal of Heat and Mass Transfer* 2015;84:1019–29. <https://doi.org/10.1016/j.ijheatmasstransfer.2014.12.046>.
- [42] Corsetti S, Miles REH, McDonald C, Belotti Y, Reid JP, Kiefer J, et al. Probing the evaporation dynamics of ethanol/gasoline biofuel blends using single droplet manipulation techniques. *J Phys Chem A* 2015;119:12797–804. <https://doi.org/10.1021/acs.jpca.5b10098>.
- [43] Uslu S, Celik MB. Combustion and emission characteristics of isoamyl alcohol-gasoline blends in spark ignition engine. *Fuel* 2020;262:116496. <https://doi.org/10.1016/j.fuel.2019.116496>.
- [44] Qian Y, Liu G, Guo J, Zhang Y, Zhu L, Lu X. Engine performance and octane on demand studies of a dual fuel spark ignition engine with ethanol/gasoline surrogates as fuel. *Energy Conversion and Management* 2019;183:296–306. <https://doi.org/10.1016/j.enconman.2019.01.011>.
- [45] Uslu S, Aydın M. Effect of operating parameters on performance and emissions of a diesel engine fueled with ternary blends of palm oil biodiesel/diethyl ether/diesel by Taguchi method. *Fuel* 2020;275:117978. <https://doi.org/10.1016/j.fuel.2020.117978>.
- [46] Uslu S. Optimization of diesel engine operating parameters fueled with palm oil-diesel blend: Comparative evaluation between response surface methodology (RSM) and artificial neural network (ANN). *Fuel* 2020;276:117990. <https://doi.org/10.1016/j.fuel.2020.117990>.
- [47] Department for Transport. *Renewable Fuel Statistics* 2019. <https://www.gov.uk/government/collections/renewable-fuel-statistics> (accessed September 20, 2019).
- [48] Kuti OA, Sarathy SM, Nishida K. Spray combustion simulation study of waste cooking oil biodiesel and diesel under direct injection diesel engine conditions. *Fuel* 2020;267:117240. <https://doi.org/10.1016/j.fuel.2020.117240>.
- [49] Al Qubeissi M, Sazhin SS, Crua C, Turner J, Heikal MR. Modelling of biodiesel fuel droplet heating and evaporation: effects of fuel composition. *Fuel* 2015;154:308–18. <https://doi.org/10.1016/j.fuel.2015.03.051>.